KIGAS Vol. 12, No. 1, March, 2008
(Journal of the Korean Institute of Gas)

Experimental Studies on the Interaction Between a Propagating Flame and Multiple Obstacles in a Rectangular Chamber

†Dal Jae Park · Jeong Jin Ahn* · Young Soon Lee**

Research Centre for System Safety, Seoul National University of Technology, Seoul 139-743, Korea
**Institute of Gas Safety R & D, Korea Gas Safety Corporation, Gyeonggi-do 429-712, Korea*
***Dept. of Safety Engineering, Seoul National University of Technology, Seoul 139-743, Korea*
(Received February 23, 2008, Accepted March 21, 2008)

Abstract – Experimental investigations were performed to assess the influences of different multiple obstacles on flame propagation in a rectangular confinement. Three different multiple obstacles were used: circular, triangular and square cross-sections with blockage ratios of 15% and 30%. The same method described in Park *et al.* [13] to investigate the interaction between the propagating flame and the obstacle was applied. Before the freely propagating flame impinged on the obstacle, the flame propagation speed remains close to the laminar burning velocity, regardless of the obstacles used. The reported data revealed that the trend in increase of the local flame propagation speed is a result of the interaction between the obstacle and the propagating flame front behind the obstacle. The local speed was found to increase from a circular to a triangular and a square obstacle. The mean flame speed was found to be less dependent on both the obstacle types and the different blockage ratios used.

Key words : Flame front, Flame displacement speed, Obstacle shapes

I. Introduction

Previous studies of flame/obstacle interactions by Moen *et al.* [1], Hjertager *et al.* [2], Urtiew *et al.* [3], Starke and Roth [4], Phylaktou and Andrews [5], Pritchard *et al.* [6], Fairweather *et al.* [7], Masri *et al.* [8], Ibrahim and Masri [9], Ibrahim *et al.* [10], and Hargrave *et al.* [11] performed in large length to diameter (L/D) ratio vessels and pipes have demonstrated the importance of obstacle geometry and blockage ratio to both the flame speeds and the explosion overpressures [11]. The interaction of the developing flow with obstacles can wrinkle the surface of a propagating flame front, and increase the flame surface area, thereby increasing the burning rate. The interaction between propagating flames and obstacles is a key phenomenon in determining the severity of turbulent gaseous explosions [12].

In previous measurements of Park *et al.* [13], experimental data were reported for the interactions of flames with different single obstacles of square, triangular, circular and rectangular cross-sections in a rectangular chamber that has a small length to diameter ratio of 0.25 and large rectangular venting. In previous measurements of Park *et al.* [14], experi-mental data were reported for interactions between a propagating flame and solid wall obstructions within the same chamber. The results reported by Park *et al.* [13,14] showed that the mean flame speeds were found to be not increasing much with blockage ratio for the same obstacle used and they were also not significantly different for different shapes at the same obstruction ratio compared to results shown in the literature for large L/D ratios.

The main reasons seem to be linked to different calculation methods of flame speed and different measurement systems. A detailed discussion of the reasons was given by the authors in those papers.

However, the effects of different multiple obstacles in flame speeds have not been examined in the explosion chamber. This paper examines the transient interactions of propagating flame with different multiple obstacles in the same chamber.

II. Experimental

The apparatus, techniques, and reactive mixture have been described in the study of Park *et al.* [13]. The methane air mixture used in all experiments was 10%. Three different multiple obstacles of circular, square and triangular bars with blockage ratios of 15 and 30% were mounted inside the chamber and centred at 117.5 mm from the bottom of the chamber. Table 1 gives the obstacle configurations.

†Corresponding author: pdj70@snut.ac.kr

Table 1. Configurations of different multiple obstacles used in the explosion chamber.

	Obstacle shapes	Symbol	Dimensions (mm)	*H* (mm)	B.R. (%)
Multiple obstacles	Cylindrical Bars	MC1	Length 950 × Diameter 50, Pitch = 250	92	15
		MC2	Length 950 × Diameter 100, Pitch = 250	67	30
	Square Bars	MS1	Length 950 × Side 50, Pitch = 250	92	15
		MS2	Length 950 × Side 100, Pitch = 250	67	30
	Triangular Bars	MT1	Length 950 × Equal sides 50, Pitch = 250	95	15
		MT2	Length 950 × Equal sides 100, Pitch = 250	74	30

Note. *H*: Distance from the bottom of chamber to the middle point of the obstacle facing the ignition point.

III. Analysis Methods of Local Flame

The steps to examine the local flame front characteristics between the flame and the multiple obstacles were the same with those described in previous work of Park *et al.* [13].

As shown in Fig. 1(a), the local region of interest selected here was around the central obstacle. Figure 1(b) shows one example of image processing applied in the area of interest to the original flame image obtained at 60 ms after ignition. The extraction of the flame front position is obtained from the processed images. Fig. 2 shows an example of local flame movement around the circular cross-section obtained at 60 ms after ignition and how the local flame displacement speed is estimated.

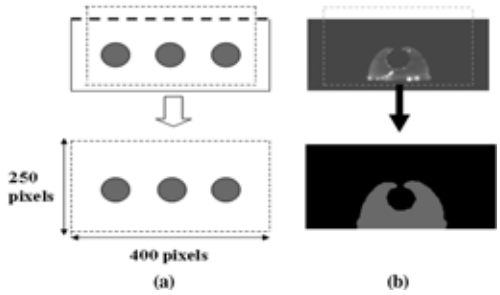

Fig. 1. (a) Selection of a local area of interest and (b) Example of image processing applied to the original flame image in the area of interest.

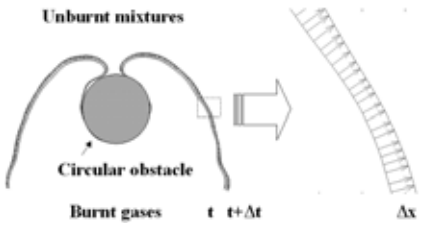

Fig. 2. Flame-front location and estimation of the local flame-front displacement.

IV. Results and Discussion

4.1. Overall Flame Propagation

Fig. 3 shows a sequence of selected high-speed images of flame propagation during the course of the explosions with multiple obstacles of circular, triangular and square cross-sections, respectively. The time shown represents the elapsed time after ignition and subsequent flame images are at 30 ms intervals.

The flame in the early stages of flame propagation is an expanding hemisphere from the central ignition point that was positioned centrally the bottom of the chamber. Before the propagating flame fronts impinge on the obstacle, the flame is entirely laminar. As the flame front propagates towards the obstacle, the gas flow ahead of the flame is pushed past the obstacle. As the flame front impinges on the front face of

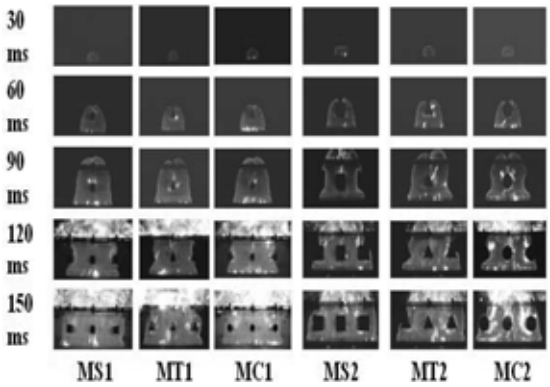

Fig. 3. A sequence of selected high-speed images of flame propagation with different multiple cross-section obstacles; square bars (MS1 & MS2), triangular bars (MT1 & MT2) and cylinders (MC1 & MC2), respectively.

obstacle, the flame becomes wrinkled due to the blockage by the obstacles and the expansion of burnt gas volume.

After impinging on the obstacle, the flame starts to propagate towards the chamber vent through the space between the obstacles. With increasing time, the leading flame starts to roll up behind the obstacle. The propagating flame fronts reconnect in the wake of the central obstacle.

After the flame reconnection behind the obstacle, the flame front approaches the chamber exit, and the flame begins to move out of the vent, allowing the unburnt fuel-air mixture to escape to the atmosphere. The propagating flame front also travels laterally along the rectangular vent with an increase in flame surface area, pushing unburnt mixture ahead of it. The interaction of flame around the obstacle with the vent caused complex vortices to form as flame spread along the obstacle towards the side of the chamber.

As indicated in Table 2, for multiple bars of 15% blockage ratio, the propagating flame fronts reached the closest face of the obstacle to the ignition point at around 30-32 ms. At 30% blockage ratio, this occurred earlier at around 26 ms after ignition.

While the flame-fronts reconnection in the wake of the square and circular bars occurred at about 54-56 ms for a 15% blockage ratio but it was relatively slower with the triangular obstacles.

However, at 30% blockage ratio, the faster flame reconnection occurred with the triangular and circular bar while the slowest flame reconnection occurred with the squares.

Following flame reconnection in the wake of the obstacle, the shortest delay time to the flame exiting the chamber at 15% blockage ratio, like the studies by Masri *et al.* [8] was the square obstacles while the longest occurred with the triangular obstacles. However, at 30% blockage ratio, the shortest time was with the triangular obstacles while the longest occurred with the circular obstacles.

Table 2. Travel time for the flame to reach the middle point of the obstacle, the flame reconnection time behind the obstacles, and the delay time for the flame to exit the chamber after ignition.

	MS1	MT1	MC1	MS2	MT2	MC2
a	30	32	32	26	26	26
b	54	60	56	72*	68*	68
c	72	78	74	68	64	74

Note. a: Travel time for the flame to reach the middle point of the obstacle (mm). b: Flame reconnection time (ms). c: The delay time for the flame to exit the chamber (ms). *: Flame-front reconnection occurs outside the chamber vent.

4.2. Statistics of Local Flame Speed

Figs. 4 and 5 show the temporal evolution of propagating flame front contours around the different multiple cross-section bars with blockage ratios of 15 and 30%.

As described in previous measurements [13,14], subsequent flame fronts are also traced with an interval of 2 ms, and the local flame displacement speed and its probability density functions (PDFs) outside the chamber exit are not included in this work. A statistical method of the PDFs of local flame displacement speed obtained through the interactions

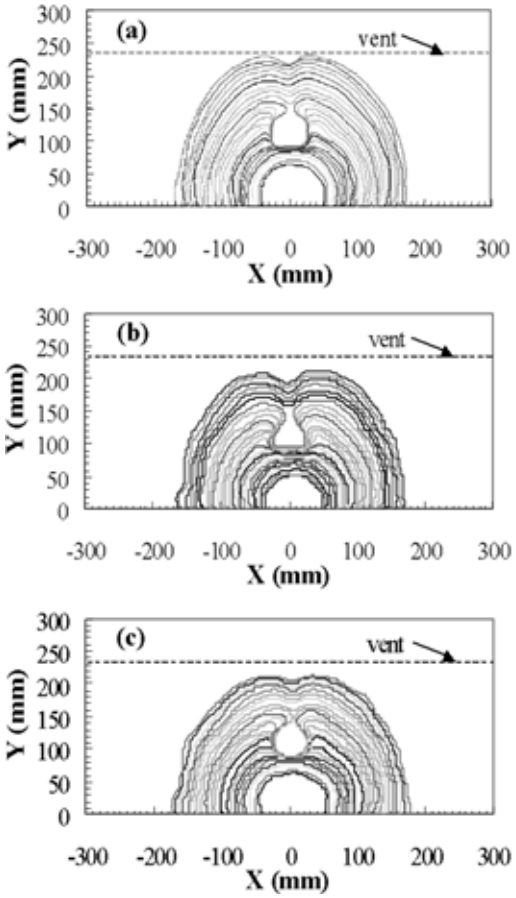

Fig. 4. Temporal evolution of flame contours (from 20 to 70 ms with time interval = 2 ms) around the central cross-sections of multiple obstacles (B.R. = 15%); (a) MS1 (square), (b) MT1 (triangle) and (c) MC1 (circle).

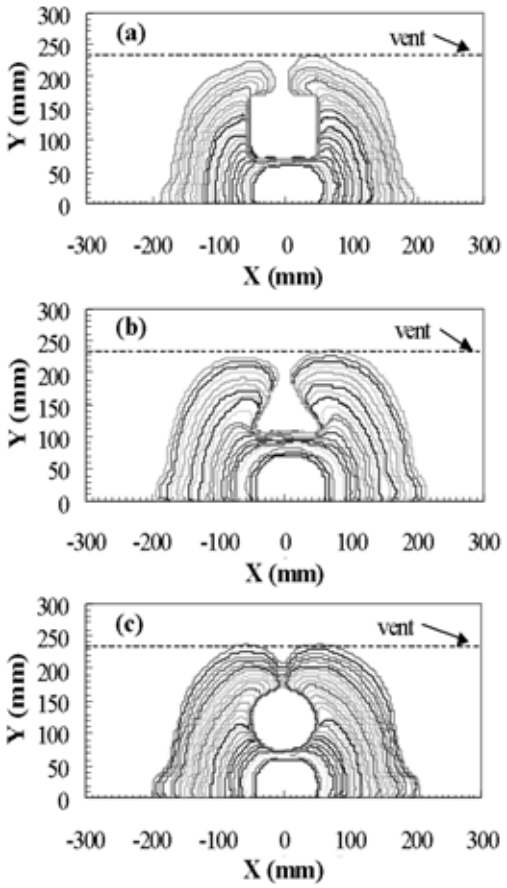

Fig. 5. Temporal evolution of flame contours (time interval = 2 ms) around the central cross-sections of multiple obstacles (B.R. = 30%); (a) MS2 (square, 20 to 64 ms), (b) MT2 (triangle, 20 to 62 ms) and (c) MC2 (circle, 20 to 74 ms).

between the moving flame fronts and the central obstacle of the multiple obstacles were exactly the same as described in the work of Park *et al.* [13]. The analysis broke to interaction into four or five stages as justified in the work of Park *et al.* [13].

The flame displacement speed PDFs for the multiple bars which have blockage ratios of 15 and 30% are seen in Figs. 6 and 7. Figs. 6(a) to (c) show the PDFs at 15% blockage ratio. All the PDFs during stage I for the different obstacles are skewed below 2.85 m/s, indicating a laminar flame value. In stage II the PDFs are still found be slightly skewed to lower displacement speeds (S_{fd} < 2.85 m/s). The PDFs during stage III only identified the flame interaction with the lateral sides of the square obstacle that are distributed to both the higher displacement speeds (S_{fd} > 2.85 m/

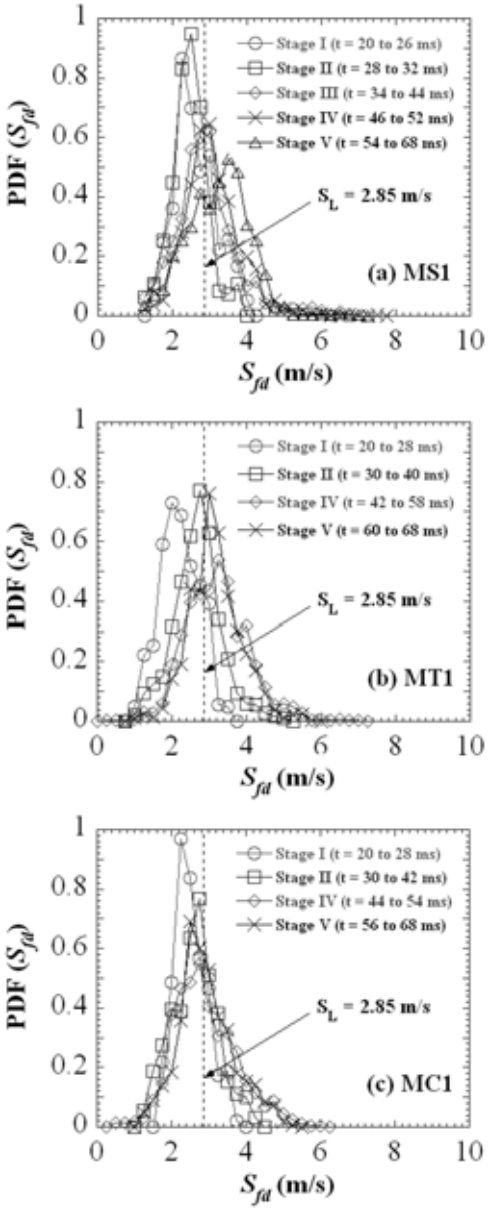

Fig. 6. PDFs of flame displacement speed around the central square, triangular and circular cross-sections of multiple obstacles with a blockage ratio of 15% at different stages: (a) MS1, (b) MT1 and (c) MC1.

s) and lower speeds (S_{fd} < 2.85 m/s). The PDFs during stage IV are skewed to the speeds (S_{fd} > 2.85 m/s). The PDFs during stage V had also a positive skewness to the speeds (S_{fd} > 2.85 m/s), the distribution widens towards higher and lower values.

The flame speed PDFs around the central obstacle

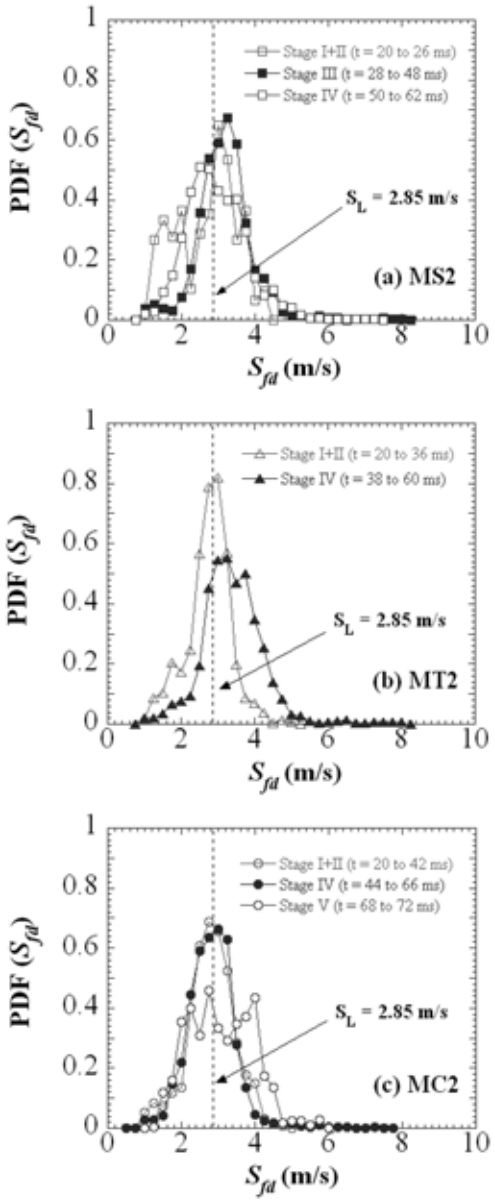

Fig. 7. PDFs of flame displacement speed around on the central square, triangular and circular cross-sections of multiple obstacles with a blockage ratio of 30% at different stages: (a) MS2, (b) MT2 and (c) MC2.

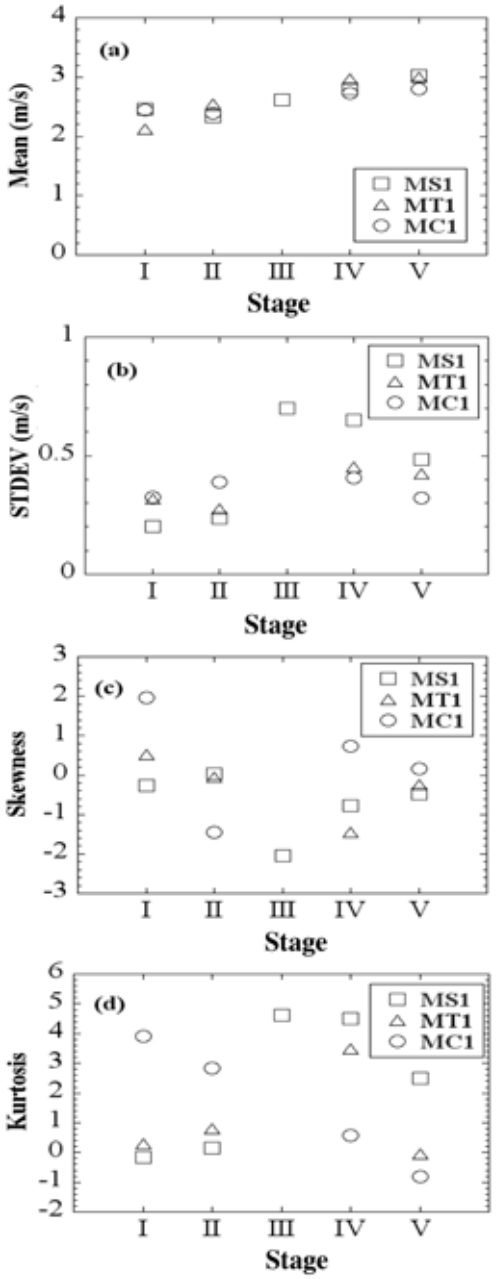

Fig. 8. Moments of the flame displacement speed PDFs for different multiple obstacles with a blockage ratio of 15% at different stages in Fig. 6; (a) mean, (b) standard deviation, (c) skewness and (d) kurtosis.

of 30% blockage ratio are shown in Figs. 7(a) to (c). Stage I+II is the link with both stage I and stage II. For the square and triangular bars, stage IV only considered up to the flame reaches the chamber exit because the flame fronts are reconnected outside the chamber exit. The stage V is not observed in the square and triangular obstacles. For large square obstacle, the PDFs show a slightly different shape during the stage I+II. As the flame front approaches

the obstacle, the central surface of the flame front becomes concave and these results in the flame deceleration in the laminar flame.

As a result two peaks occur in the PDFs of this stage: the first peak at lower speeds is linked to the flame deceleration in the laminar flame and the second peak is the normal laminar flame speed.

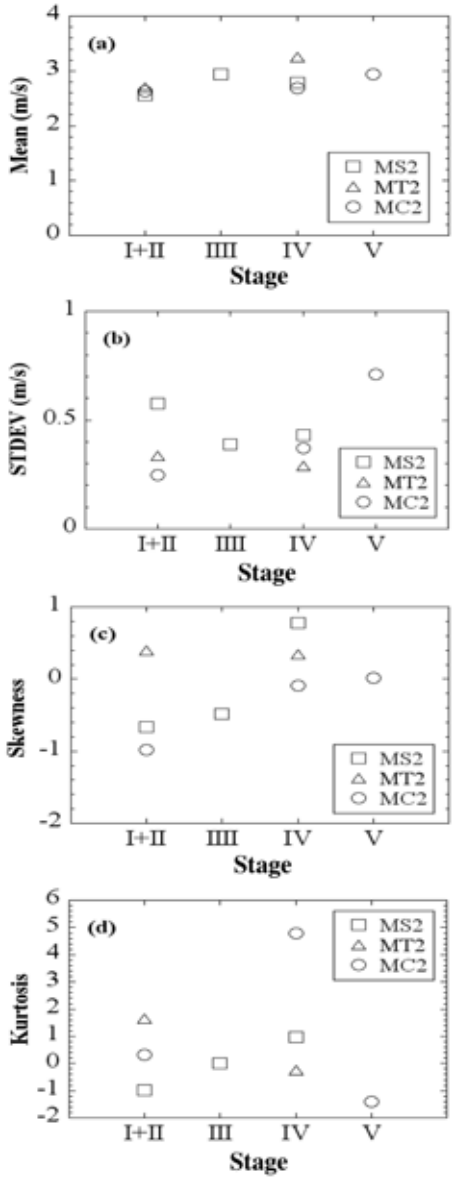

Fig. 9. Moments of the flame displacement speed PDFs for different multiple obstacles with a blockage ratio of 30% at different stages in Fig. 7; (a) mean, (b) standard deviation, (c) skewness and (d) kurtosis.

The pdf distributions at the higher blockage ratio during the stage III are similar for those of the lower blockage ratio. However, the PDFs have a slightly longer tail to higher values. The general patterns of the PDFs of flame displacement speed at the higher obstruction ratio during the stage IV for each obstacle are similar for those of the lower obstruction ratio.

The moments of the mean, standard deviation, skewness and kurtosis of the flame speed PDFs for each stage are seen in Figs. 8 and 9 for the two blockage ratios. The statistics in each were similar to those found in the tests of Park *et al.* [13].

The mean displacement speed was found to become slightly increasing. However, the mean local flame displacement speed for each obstacle was less sensitive to each stage. Also, the standard deviation in the displacement speed of each stage was generally distributed towards less than 0.5 m/s. At each stage, the skewness is generally distributed towards less than zero while the kurtosis is generally distributed towards higher than zero.

4.3. Mean Local Flame Speed

Figs. 10(a) and (b) show the temporal variations of the mean local flame displacement speed, $\overline{S_{fd}}$, for the three multiple obstacles and the two blockage ratios of 15 and 30%. For the smaller obstacles, the mean flame speed increases from about 2.2 m/s to 3.4 m/s with the square obstacle, from about 2.1 m/s to 3.3 m/s with the triangular obstacle and from about 2.2 m/s to 3.2 m/s with the circular obstacle. For the larger obstacles, the relative higher flame was observed with the square and triangular bars where the flame was found to be increased from about 2.6 m/s to 3.7 m/s and from 2.5 m/s to 3.6 m/s compared with 2.4-3.1 m/s for the circular bars. The mean flame displacement speeds around the different obstacle obstructions, resulting from weak turbulence conditions, were less dependent of the obstacle shapes and the obstruction ratios used. As the obstruction ratio within obstacles of the same shape increased, the significant differences are that the earlier development with the square, i.e. the flame goes up the sides, the later development around the triangle corresponding to the maximum width and shear layer formation and the relative flatness of the circular one.

When flame speeds obtained from single obstacles used by Park *et al.* [13] were compared, even though the number of obstacles is different, the general trend of the mean flame speeds is with any differences being not significant, excepting for the larger square obstacle,

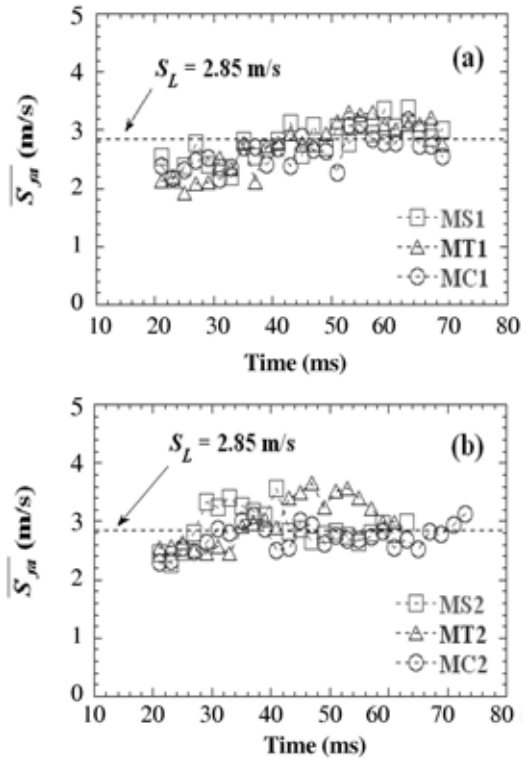

Fig. 10. Temporal evolution of the mean flame displacement speed after ignition for (a) small multiple bars (MS1, MT1 and MC1) and (b) large multiple bars (MS2, MT2 and MC2).

causing the faster increase as the flame goes up the sides. The flame speeds around the central obstacle were found to be almost less dependent of the number of obstacles from single to multiple.

V. Conclusions

Experimental studies have been carried out to investigate the influence of different multiple bars within the chamber with a small L/D ratio of 0.25 and a large rectangular vent. Three different obstacles of square, cylindrical and triangular cross-sections covering blockage ratios of 15 and 30% were used. The main results obtained from the present work are summarized as follows:

1. The early flame propagation for all the obstacles used was an expanding hemispherical laminar flame from the ignition point. Flame reconnection occurs faster for the same obstacle configuration at a smaller blockage ratio but reaches the chamber exit earlier at the larger blockage ratio.

2. The local flame displacement speed PDFs during the stage IV, representing the flame interaction with the modified flow formed behind the obstacle were extensively distributed towards higher displacement speed. The averaged flame displacement speeds around the obstacles were less sensitive to the obstacle shapes and the obstruction ratios used. When single and multiple obstacles were compared, the mean flame displacement speed was also found to be less sensitive to the number of obstacles of a given width.

References

[1] Moen, I.O., M. Donato, R. Knystautas and J.H.S. Lee, "Flame Acceleration Due to Turbulence Produced by Obstacles", *Combustion and Flame*, **39**, 21-32, (1980)

[2] Hjertager, B.H., K. Fuhre, and M. Bjorkhaug, "Concentration Effects on Flame Acceleration by Obstacles in Large-scale Methane-air and Propane-air Vented Explosions", *Combustion Science and Technology*, **62**, 239-256, (1988)

[3] Urtiew, P.A., J. Brandeis and W.J. Hogan, "Experimental study of Flame Propagation in Semi-confined Geometries with Obstacles", *Combustion Science and Technology*, **30**, 105-119, (1983)

[4] Starke, R. and P. Roth, "An Experimental Investigation of Flame behavior during Explosions in Cylindrical Enclosures with Obstacles", *Combustion and Flame*, **75**, 111-121, (1989)

[5] Phylaktou, H. and G.E. Andrews, "Gas Explosions in Long Closed Vessels", *Combustion Science and Technology*, **77**, 27-39, (1991)

[6] Pritchard, D.K., D.J. Freeman and P.W. Guilbert, "Prediction of Explosion Pressures in confined Spaces", *Journal of Loss Prevention in the Process Industries*, **9**, 205-215, (1996)

[7] Fairweather, M., G.K. Hargrave, S.S. Ibrahim and D.G. Walker, "Studies of Premixed Flame Propagation in Explosion Tubes", *Combustion and Flame*, **116**, 504-518, (1999)

[8] Masri, A.R., S.S. Ibrahim, N. Nehzat and A.R. Green, "Experimental study of Premixed Flame Propagation Over Various Solid Obstructions", *Experimental Thermal and Fluid Science*, **21**, 109-116, (2000)

[9] Ibrahim, S.S. and A.R. Masri, "The effects of Obstructions on Overpressure Resulting from Premixed Flame Deflagration", *Journal of Loss Prevention in the Process Industries*, **14**, 213-221, (2001)

[10] Ibrahim, S.S., G.K. Hargrave, and T.C. Williams, "Experimental Investigation of Flame/solid Interac-

tions in Turbulent Premixed Combustion", *Experimental Thermal and Fluid Science*, **24**, 99-106, (2001)

[11] Hargrave, G.K., S.J. Jarvis and T.C. Williams, "A study of Transient Flow Turbulence Generation During Flame/wall Interactions in Explosions", *Meas. Sci. Technol.*, **13**, 1036-1042, (2002)

[12] Lindstedt, R.P. and V. Sakthitharan, "Time Resolved Velocity and Turbulence Measurements in Turbulent Gaseous Explosions", *Combustion and Flame*, **114**, 469-483, (1998)

[13] Park, D.J., A.R. Green, Y.S. Lee and Y.C. Chen, "Experimental studies on Interactions between a Freely Propagating Flame and Single Obstacles in a Rectangular Confinement", *Combustion and Flame*, **150**, 27-39, (2007)

[14] Park, D.J., T.S. Lee and Y.S. Lee, "Interactions between a Freely Propagating Flame and Rectangular Obstacles in a Rectangular Confinement", Asia Pacific Symposium on Safety, 30 October-2 November, Busan, Korea, 103-107, (2007)